Journal of Inclusion Phenomena and Molecular Recognition in Chemistry **16:** 139–153, 1993.

Hydrothermal Synthesis of Al- and Ga-Substituted Omega Zeolite

S. P. MIRAJKAR, M. J. EAPEN, S. S. TAMHANKAR, B. S. RAO and V. P. SHIRALKAR*
Catalysis Division, National Chemical Laboratory, Pune – 411 008, India.

(Received: 19 May 1993; in final form: 21 September 1993)

Abstract. The synthesis and characterisation of zeolite Al- and Ga-Omega has been studied in the temperature range 383–413 K using tetramethyl ammonium hydroxide as a template. The evidence for framework gallium substitution was obtained from chemical analysis, X-ray diffraction, IR, solid state MAS NMR, thermoanalytical studies and ion exchange. Crystal morphology varied with the degree of isomorphous substitution of both Al and Ga and the synthesis temperature.

Key words: Synthesis, Al-Omega, Ga-Omega, crystallisation kinetics, X-ray diffraction, IR, MAS NMR, sorption.

1. Introduction

Zeolite omega (ZSM-4) is a synthetic counterpart to the mineral mazzite. The aluminosilicate framework consists of columns of gmelinite cages bridged by oxygen atoms to give a 12-membered cylindrical main channel system along the crystallographic c axis [1–3]. The zeolite is usually crystallised at 363–423 K from aluminosilicate hydrogels containing a mixture of sodium and tetramethylammonium hydroxide (TMA-OH) ions [4–11].

The isomorphous replacement of Al by other trivalent cations in the zeolite framework has been reviewed by Barrer [12], Szostak [13] and others [14]. The gallium analogues of zeolites possess physical and chemical properties different from their aluminium analogues [15]. The gallium analogues of ZSM-5 [16], EU-1 [17], mordenite [18] and Y [19] have already been documented. Omega zeolite ($SiO_2/Al_2O_3 = 7–8$) possesses excellent thermal, hydrothermal and acid stability. Isomorphous substitution of gallium for aluminium in the omega framework may produce [20, 21] a novel catalyst with interesting applications. The results on the synthesis and characterisation of Al-omega and Ga-omega are reported in this paper.

* Author for correspondence.

2. Experimental

2.1. Synthesis

Synthesis of omega (Al) was carried out hydrothermally using silica sol (28.9% SiO_2), tetramethylammonium hydroxide (TMA-OH) (25% w/w in methanol), sodium aluminate (39% Na_2O, 43% Al_2O_3), sodium hydroxide and distilled water. A solution containing 1.17 g of sodium aluminate and 2.0 g of sodium hydroxide in 10 g of distilled water was mixed with 1.6 g of tetramethylammonium hydroxide. This solution was slowly added with vigorous stirring to 18.0 g of silica sol. The thick paste formed was converted into uniform slurry by continuously stirring for a few hours. The gel slurry, having the following composition in terms of oxide mole ratio, was transferred to a stainless steel autoclave and heated up to 383–413 K for 5–20 days.

$$6.78\ Na_2O : Al_2O_3 : 17\ SiO_2 : 0.43\ (TMA)_2O : 251\ H_2O\ .$$

Samples were taken at different crystallisation times in order to monitor the progress of crystallisation. The autoclave was removed from the oven and quenched under cold water. The crystalline white solid was filtered, washed and dried at 393 K in air for 6 h. The X-ray powder diffraction pattern confirmed that the product was a highly crystalline aluminosilicate having the omega structure. The gallosilicate analogue was prepared with the same oxide molar composition, except that anhydrous gallium nitrate was used in place of sodium aluminate, which necessitated the addition of a calculated quantity of sodium hydroxide to match with the sodium content in the Al-omega gel.

2.2. Characterisation

The chemical composition and physicochemical characterisation of the various omega samples were determined by various techniques. The crystalline phase identification was done with XRD (Rigaku, D/Max-III VC) using CuK_α radiation ($\lambda = 1.5481$ Å). The crystal habit and morphology were studied using a JEOL JSM 5200 scanning electron microscope by coating the sample with an evaporated Au film on an aluminium sample holder. Simultaneous thermoanalytical curves (DTA and TG) were obtained in air with a Setaram TG-DTA 92 analyser. Framework IR vibration spectra (Pye-Unicam, SP 300) were recorded by using the Nujol mull technique. The solid state MAS NMR spectra (^{29}Si, ^{27}Al and ^{71}Ga) were recorded at 298 K on a Bruker-MSL-300 FT NMR spectrometer. For ^{29}Si spectra, a 2s pulse and a recycle time of 3s were found to be sufficient and the chemical shift was measured with respect to tetramethylsilane (TMS) as an external reference. For ^{27}Al spectra a 3s pulse and a 0.25s recycle time were found to be adequate and the aqueous solution of $AlCl_3$ served as an external reference. For ^{71}Ga a 3s pulse and a 0.3s recycle time were found to be sufficient and $[Ga(H_2O)_6]^{3+}$

was used as an external reference. The sorption measurements were carried out using a conventional gravimetric system consisting of a McBain balance. The equilibrium sorption capacities were measured at $P/P_0 = 0.8$ and 298 K (up to 2 h) on samples degassed at 673 K under a vacuum of the order of 10^{-6} Torr. The chemical compositions of the products were obtained by a combination of wet chemical, atomic absorption (Hitachi Z-8000) and ICP (Jobin-Yvon – JY-38 VHR) methods. The ion exchange properties of Ga-omega were evaluated by saturating the calcined (organic-free) gallosilicate sample with 1.0N NaCl solution and then by ion exchanging with potassium. Ion exchange was done under reflux at 368 K for 4 h. The procedure was repeated to ensure complete ion exchange.

3. Results and Discussion

3.1. X-Ray Diffraction and Crystallisation Kinetics

Figure 1 shows the XRD patterns of Ga-omega and Al-omega zeolites. The XRD pattern of Al-omega is in close agreement with the reported data [7]. There is also a close similarity between the XRD patterns for Al-omega and Ga-omega. Table I clearly indicates a lowering of 2θ values for the XRD reflections in Ga-omega as compared to those in Al-omega; and this may be a consequence of an incorporation of the comparatively larger gallium species in place of framework aluminium. A similar expansion has also been reported after the isomorphous substitution of Ga into the framework of mordenite [18]. The unit call volume calculated from the XRD data for Ga-omega (2545 $Å^3$) is higher than that for Al-omega (2519 $Å^3$) as summarised in Table I. This observation is also consistent with Ga-O bonds being longer than Al-O bonds.

The crystallisation kinetics were studied by comparing the extent of crystallisation of the gel mixture at different intervals of synthesis time at different temperatures. The crystallisation kinetic curves (shown in Figure 2) at 383, 398 and 413 K were obtained by measuring percentage crystallinity and by the ratio of the sum of areas [22] of intense peaks of the sample under consideration to that of the most crystalline sample obtained during the studies. The curves exhibit a sigmoidal or S-shaped nature, indicating different rates of crystallisation at different synthesis times. We define the initial portion (induction period) as corresponding to the time needed to form crystallisation centres or nuclei. This is followed by the rapid formation of the crystalline structure. Lastly, the rate of crystallisation decreases as the process approaches completion, indicated by a near-constancy (100%) in percentage crystallisation.

3.2. SEM

The progress in crystallisation has also been monitored by scanning electron micrography. Figure 3 shows that, as the degree of crystallinity increases, well-defined crystallites start appearing in place of amorphous material. Figure 3 D

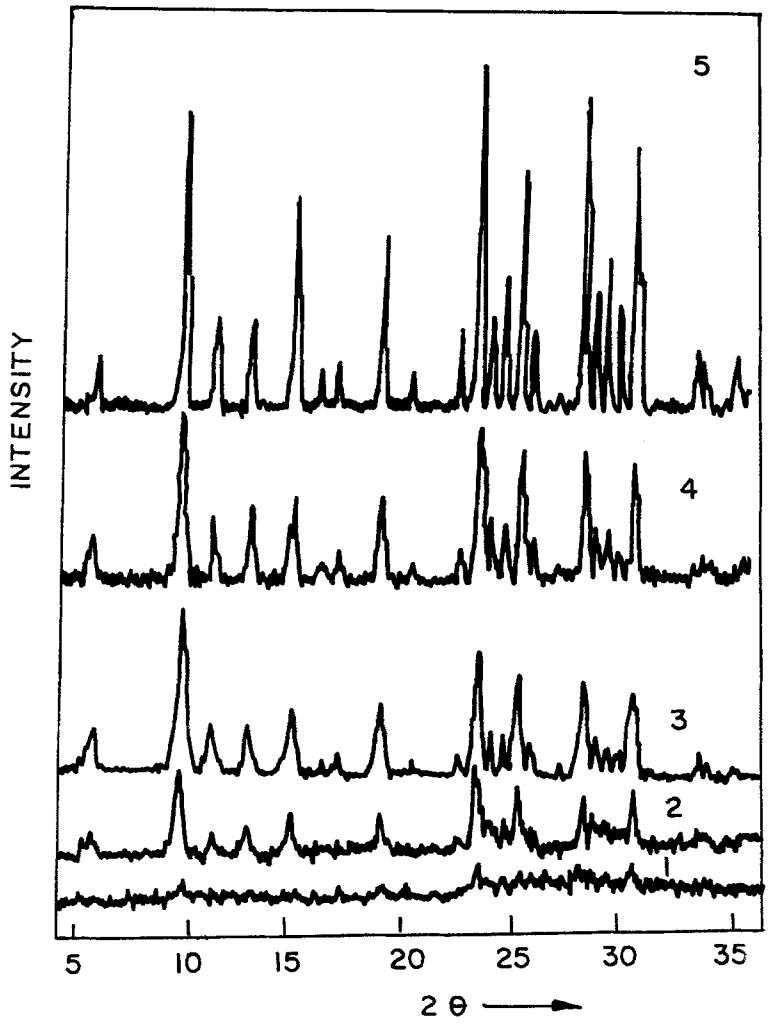

Fig. 1. XRD pattern for the Al-omega samples with different degrees of crystallinity (1) 0%, (2) 26%, (3) 72%, (4) 100% and (5) 100% Ga-omega.

shows nearly spherical crystals of size 4–5 μm for Al-omega crystallised at 398 K. The salient feature of the SEM microphotographs in Figure 3 is the change in crystal morphology for Ga-omega crystallised at 398 K. These crystallites are of cylindrical shape with average size being 4 × 2 μm for 30 h at 398 K (Figure 3 E) and 8 × 2 μm for 90 h at 398 K (Figure 3 F) and this shape is distinctly different from Al-omega crystallites. This shows a marked influence on the crystal morphology of isomorphous replacement of Al^{3+} by Ga^{3+} in the omega framework [20, 21]. Figures 3 E and 3 F also show the influence of crystallisation period on the size of crystallite. A similar change in crystal morphology [23] has also been reported in the synthesis of a number of zeolites, including omega. This shows that,

TABLE I. 'd' Spacings and relative intensities for omega samples.

Al-omega (uc volume = 2519 Å^3)				Ga-omega (uc volume = 2545 Å^3)	
Literature*		Present study		Present study	
d(Å)	$(I/I_{max}) \times 100$	d(Å)	$(I/I_{max}) \times 100$	d(Å)	$(I/I_{max}) \times 100$
9.09	86	9.089	100	9.134	100
7.87	21	7.891	17	7.916	19
6.86	27	6.878	58	6.888	23
5.94	32	5.955	47	5.979	63
4.695	32	4.690	29	4.708	21
3.794	58	3.790	87	3.805	66
3.708	30	3.704	35	3.714	14
3.62	25	3.621	33	3.628	33
3.516	53	3.518	78	3.526	37
3.456	20	3.428	25	3.441	12
3.13	38	3.141	68	3.162	71
3.074	21	3.082	35	3.094	22
—	—	3.034	30	3.043	36
—	—	2.979	17	2.988	25
2.921	63	2.924	60	2.924	60

* Ref. [28].

along with the parameters such as the nature of the ingredients, gel composition and crystallisation temperature, isomorphous species in the silica matrix exert an influence on the crystal morphology of the zeolite produced.

3.3. Framework IR Spectra

Framework IR spectra in the region 400–1300 cm^{-1} are compared for Al- omega and Ga-omega in Figure 4. A progression in crystallinity is also shown in Figure 4 by the IR spectra of Al-omega obtained at different crystallisation times. Figure 4 A shows the IR spectrum for almost amorphous (percentage crystallinity $\sim$ 10) aluminosilicate gel. As the percentage crystallinity of the product increases a very broad band at 1060 cm^{-1}, due to the asymmetric stretch, becomes sharper and shifts towards lower wavenumber (1030 cm^{-1}) in fully crystalline Al-omega (Figure 4 E) zeolite. Similarly, a shoulder band around 1105 cm^{-1} becomes more prominent around 1130 cm^{-1} in the fully crystalline sample. A band around 852 cm^{-1}, present in the amorphous sample, disappears in crystalline Al-omega. A salient feature of Figure 4 is the emergence of peaks at 820 and 620 cm^{-1} on account of absorption of structure-sensitive bands due to the symmetric stretch

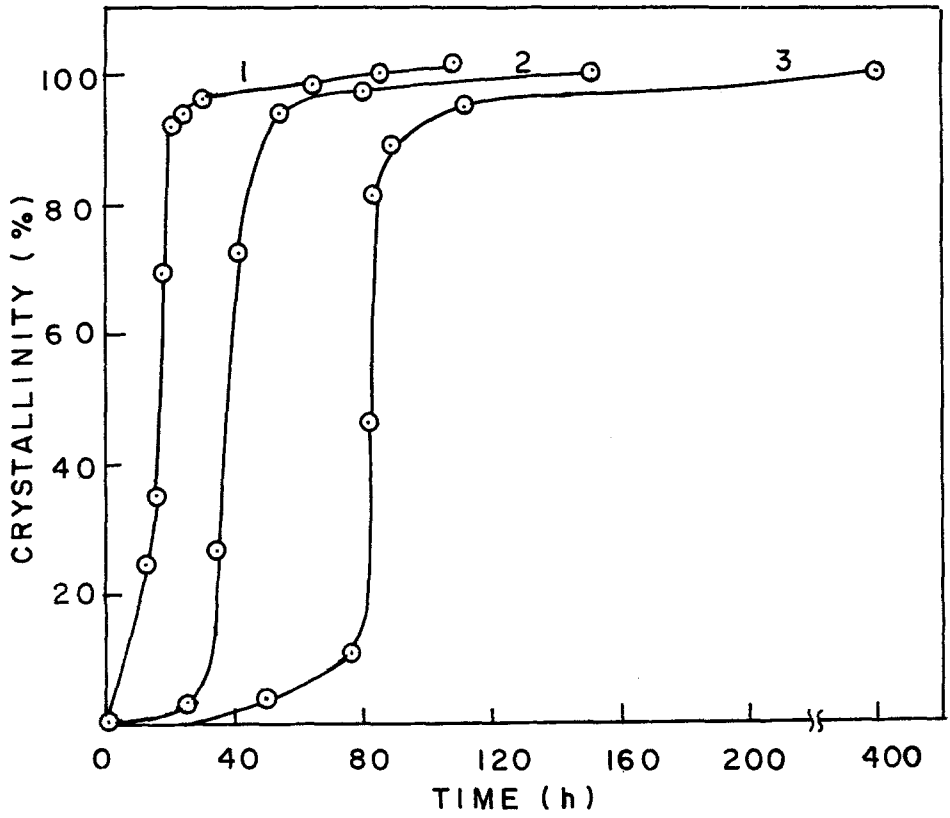

Fig. 2. Kinetics of crystallisation of Al-omega at (1) 413 K, (2) 398 K, and (3) 383 K.

and the double ring, respectively. Although the position of these bands does not shift, their intensity increases with the increase in percentage crystallinity, except for a band around 615 cm^{-1} due to a double ring which becomes very weak in Ga-omega. Also, the position of a band assigned to pore opening around 450–460 cm^{-1} does not change with crystallinity. The framework IR characteristics for Al-omega summarised in Table II are in close agreement with the reported data [24]. Another interesting feature of Figure 4 and Table II is the lower wavenumber value of all the structure-sensitive bands in Ga-omega as compared to those for Al-omega. This is in accordance with the substitution of Al^{3+} species by the heavier Ga^{3+} species in the omega framework. Sometimes a doublet around 800 cm^{-1} in the gallium analogue in place of a singlet in the aluminium analogue confirmed [25] lattice incorporation of Ga^{3+} in the omega framework.

3.4. Chemical Composition

The chemical composition of fully crystalline Al-omega and Ga-omega in the anhydrous form, determined by both gravimetric (destructive) and by XRF (non-

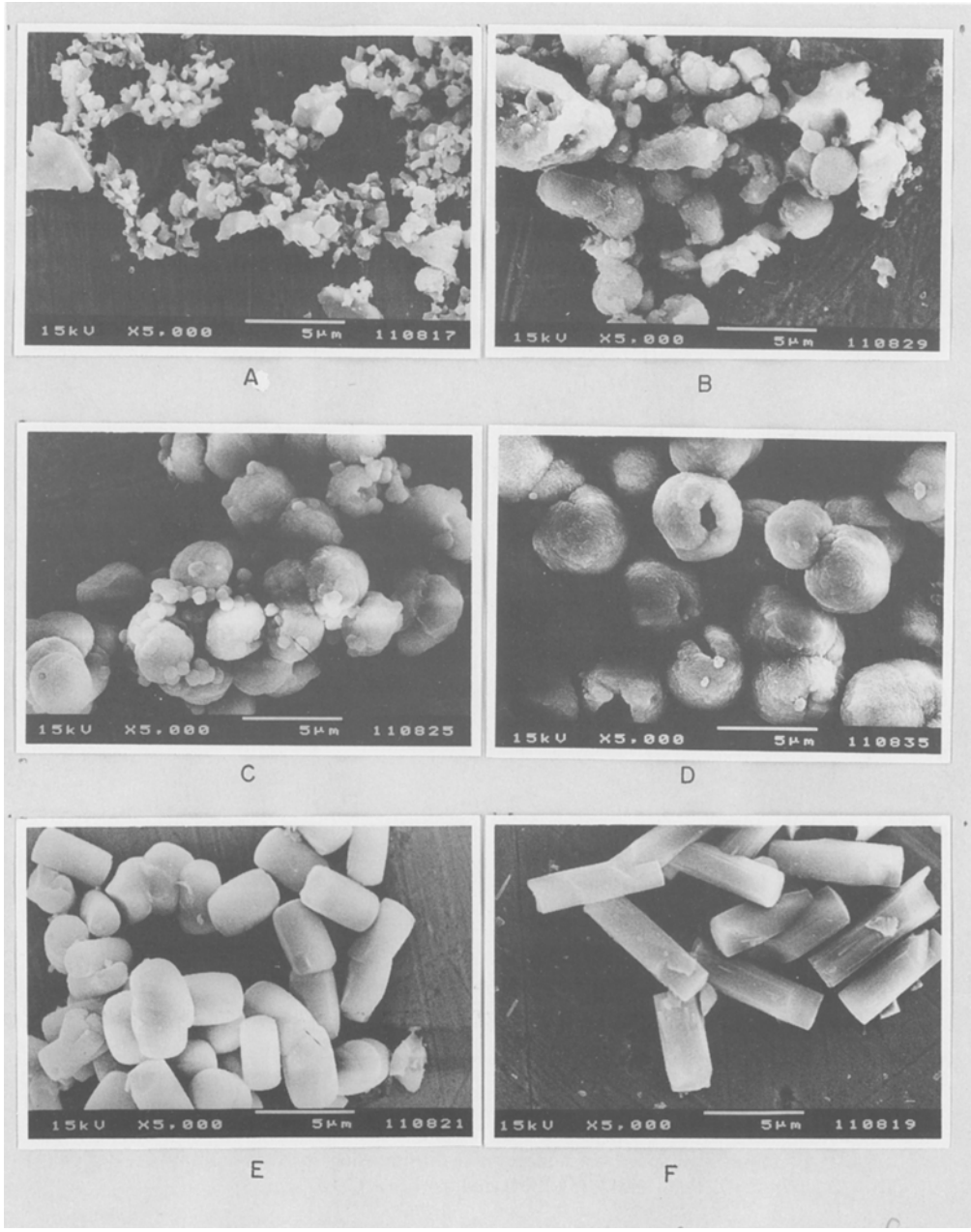

Fig. 3. SEM photographs of Al-omega samples with different degree of crystallinity (A) 26%, (B) 72%, (C) 100% at 398 K, (D) 100% at 413 K, (E) 100% Ga-omega at 398 K (20 h), (F) 100% Ga-omega at 398 K (90 h).

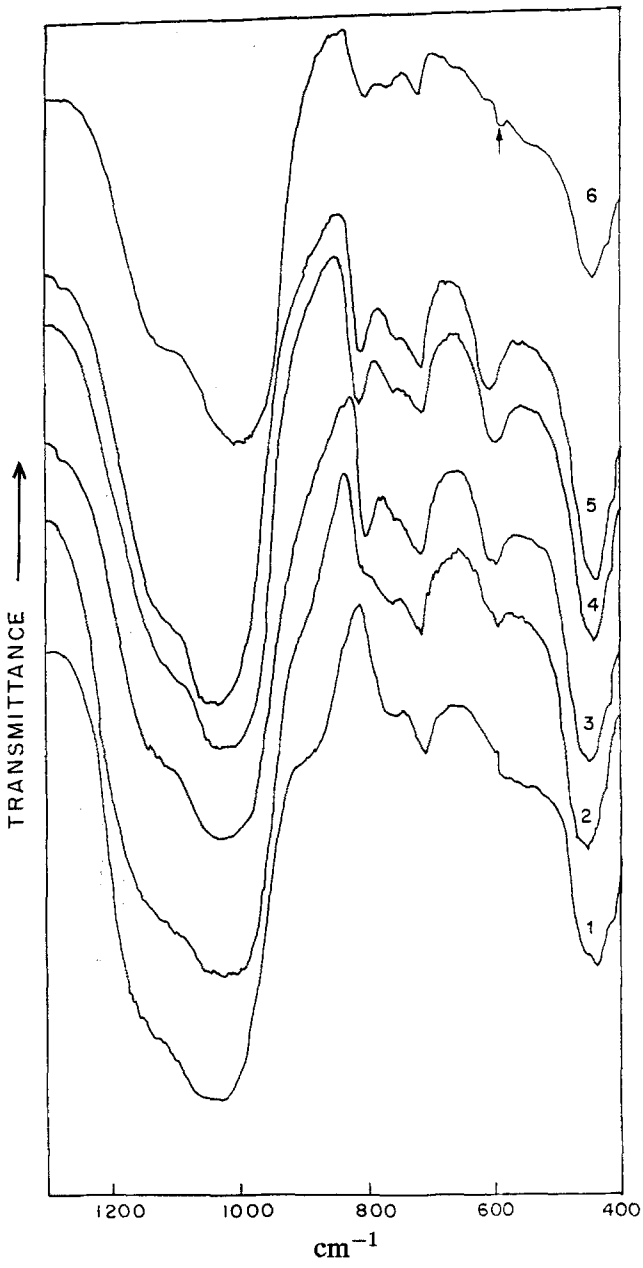

Fig. 4. Framework IR spectra of samples with different degree of crystallinity. Al-omega (1) 0%, (2) 26%, (3) 72%, (4) 93%, (5) 100% and (6) 100% Ga-omega.

destructive) methods, are compared in Table III. The silica-to-alumina ratio in the solid is found to be around 7.0 ± 0.25. The sodium occupancy, however, is only 70% of the total aluminium incorporation. This shows that the excess negative charge on 30% of framework AlO_4^- tetrahedra is balanced by protons produced upon the

TABLE II. Framework IR vibrational bands of crystalline Al- and Ga-omega.

Al-omega (synthesised at 398 K)		Al-omega* (Literature data)		Ga-omega (synthesised at 398 K)	
1130	sh	1130	sh	1139	sh
1037	vs	1024	vs	1025	vs
825	m	805	mw	815	m
770	sh	—		770	sh
730	mw	722	mw	730	mw
625	m	610	mw	615	vw
455	ms	451	ms	450	ms

* Ref. [24].
vs – very strong, sh – shoulder,
m – medium, mw – medium weak,
ms – medium strong, vw – very weak.

TABLE III. Chemical composition of Al- and Ga-omega zeolite.

Chemical composition (anhydrous)	Al-omega		Ga-omega	
	XRF	Gravimetric	XRF	Gravimetric
$\%SiO_2$	75.71	74.10	66.66	62.66
$\%Al_2O_3$	17.75	18.37	0.09	0.09
$\%Ga_2O_3$	—	—	25.82	28.71
$\%Na_2O$	7.25	7.53	7.42	8.53
$SiO_2/[Al_2O_3 + Ga_2O_3]$	7.25	6.85	7.42	6.87
Surface area, m^2g^{-1}	229		223	

decomposition of templating species. The chemical composition of Ga-omega also shows the SiO_2/Ga_2O_3 ratio to be around 6.87–7.42. The sodium occupancy in Ga-omega is 90% of the total gallium content in the solid and it is higher than that in Al-omega. The aluminium content (as an impurity from raw materials) in Ga-omega is negligible ($SiO_2/Al_2O_3 > 1200$). Since Ga-omega exhibits an XRD pattern characteristic of the omega framework with no report of Al-omega with $SiO_2/Al_2O_3 \simeq 1200$, it is reasonable to assume the incorporation of Ga^{3+} ions into the omega framework.

3.5. Solid State MAS NMR Spectroscopy

Figure 5 depicts ^{29}Si and ^{27}Al MAS NMR spectra of Al- and Ga- omega, and the ^{71}Ga MAS NMR spectrum of Ga-omega. The ^{29}Si spectra for Al- and Ga-omega are almost identical exhibiting peaks at 92.85 ppm (Si-0Al), 97.99 ppm (Si-1Al), 104.05 ppm (Si-2Al) and 111.59 ppm (Si-3Al). These NMR data are in close agreement with those reported earlier [26, 27]. The intensity of peaks corresponding to (Si-1Al) and (Si-2Al) is more than that for (Si-0Al) and (Si-3Al). The ^{27}Al MAS NMR spectrum for Al-omega shows a sharp doublet in the range 62–56 ppm, corresponding to the tetrahedral aluminium atoms located in the two non-equivalent crystallographic sites of the framework corresponding to the four-membered (S4R, site A) and six-membered rings (S6R, site B) of the gmelinite columns [26, 27]. The area under each of the peaks gives [26, 27] almost the quantitative measure of the number of these sites and the ratio Al_A/Al_B is usually around 1.25. However, the ^{27}Al MAS NMR spectrum for Ga-omega shows the absence of any significant amount of aluminium in the samples. The ^{71}Ga MAS NMR spectrum of Ga-omega shows the signal at 156.9 ppm and thus confirms the tetrahedral coordination of Ga^{3+} species in the omega framework. The gallium signal peak is not sharp but rather broad, indicating that although the sample is highly crystalline, a distortion in the symmetry around Ga nuclei may be present.

3.6. Thermal Properties

Figure 6 shows the DTA and TG curves for typical Al-omega and Ga-omega zeolites crystallised at the same temperature. Both the TG curves show a loss in weight up to 573 K (around 10 wt.-%) due to dehydration of physically sorbed water. It is then followed by a very slow loss in weight (around 1.5 wt.-%) up to 833 K, probably due to the decomposition of physically occluded template molecules. A very sharp loss in weight (around 3.5 wt.-%) takes place over a very narrow temperature range (863–893 K) due to the oxidative decomposition of templating species associated with the framework aluminium tetrahedra to balance its negative charge. After 890 K there is no more loss in weight, even up to 1273 K. The total loss in weight up to 1273 K with Al-omega is 14.5–15 wt.-% and is rather higher than that (11.5 wt.-%) in Ga-omega.

The DTA curves reflect the TG changes. A broad and weak endotherm up to 573 K due to dehydration of physically sorbed water is followed by a weak and diffuse exotherm up to 773 K due to decomposition of physically occluded template species. A very sharp exotherm in the range 880–890 K is exhibited on account of the oxidative decomposition of templating species associated with the charge compensation on the framework aluminium tetrahedra. The Ga-omega sample also gives the maximum for this exotherm at 878 K. It is seen clearly from Figure 6 that no exotherm due to structural collapse is seen at least up to 1273 K. This means that the frameworks of both Ga- and Al-omega are stable at least up to 1273 K.

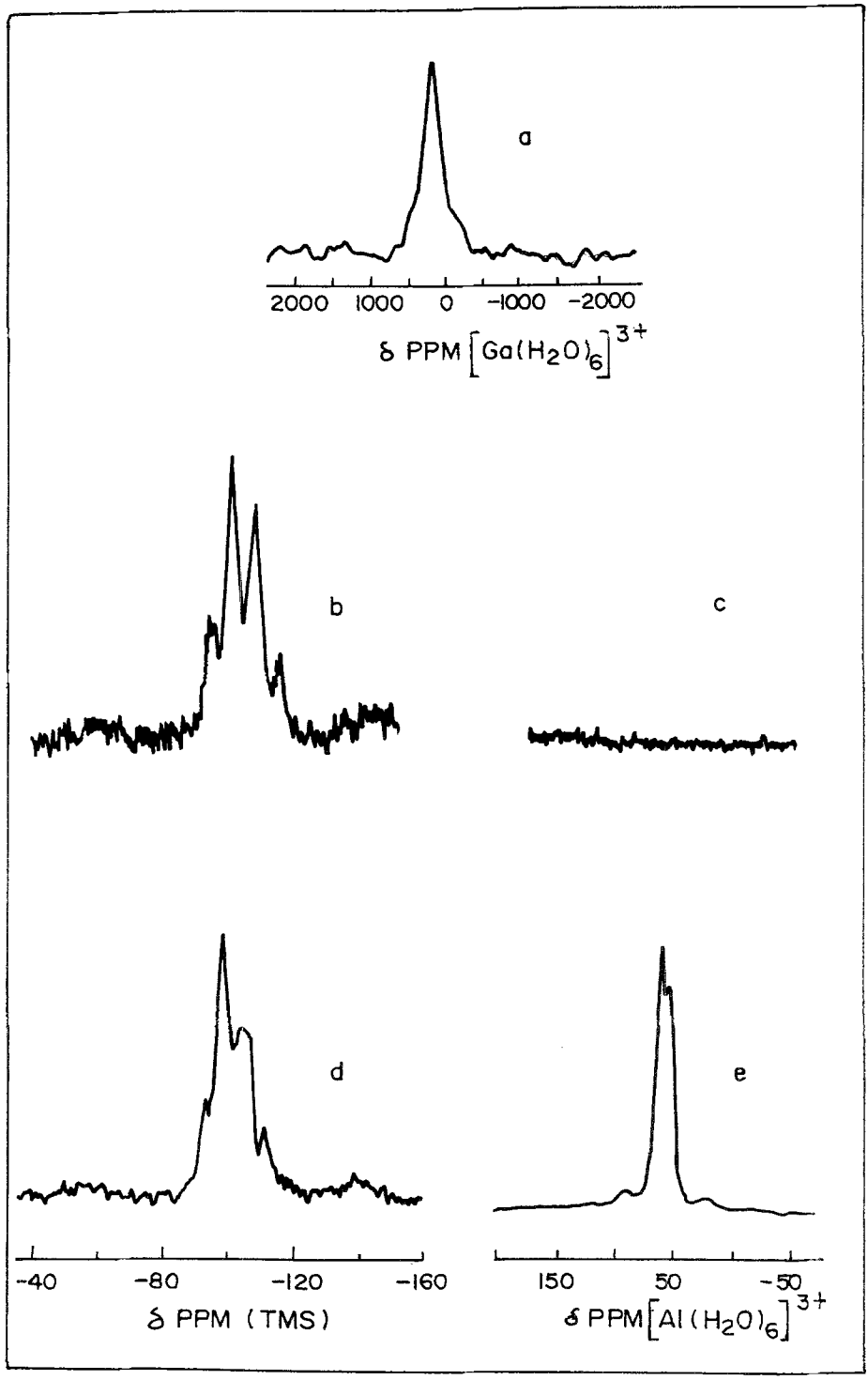

Fig. 5. MAS NMR spectra for Ga-omega of (a) ^{71}Ga, (b) ^{29}Si, (c) ^{27}Al and for Al-omega of (d) ^{29}Si and (3) ^{27}Al.

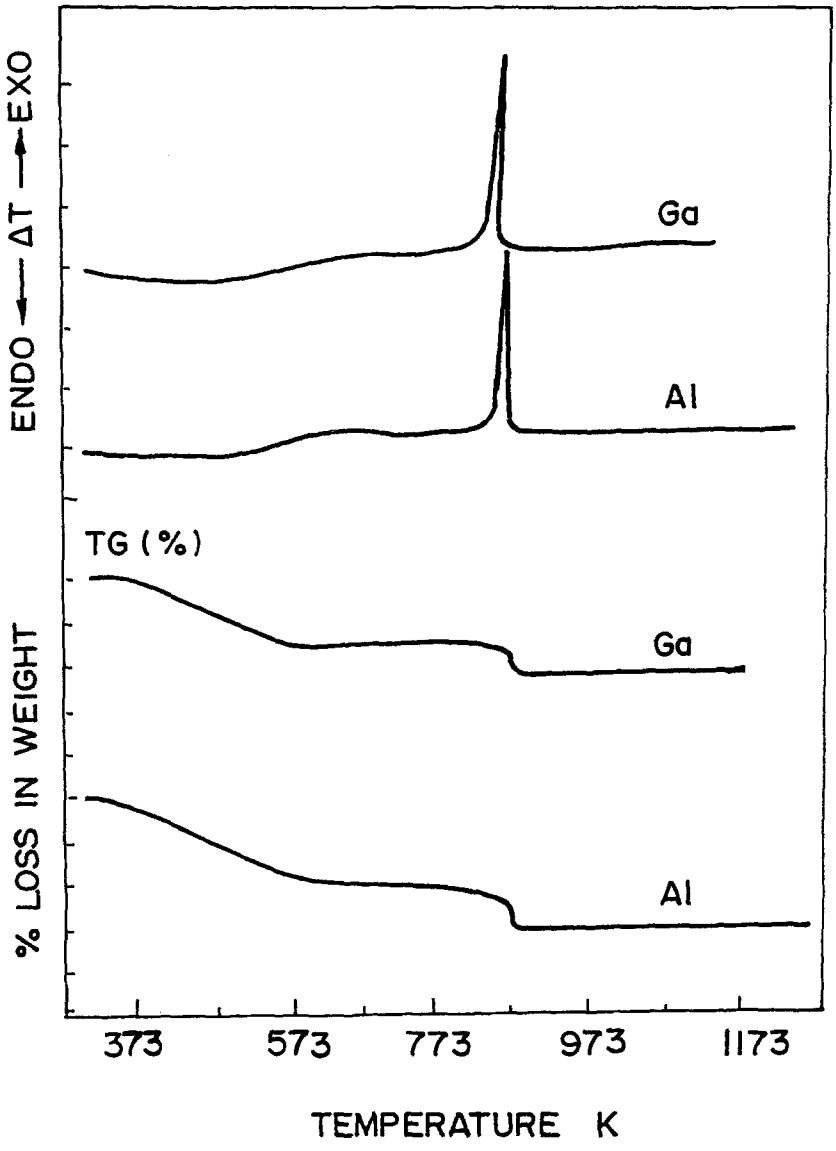

Fig. 6. Thermo-analytical (TG and DTA) curves for Al-omega and Ga-omega crystallised at 398 K.

3.7. Sorption Properties

Figure 7 depicts the sorption uptakes ($P/P_0 = 0.8$, 298 K) of samples of different crystallinity obtained from typical synthesis experiments (398 K) for Al-omega and Ga-omega. These curves typically show that sorption uptake increases as the degree of crystallinity increases. Water, being a polar molecule and comparatively small in size, is able to become occluded in cavities of samples of low crystallinity.

TABLE IV. Adsorption (wt.-%) on Al- and Ga-omega zeolites. $P/P_0 = 0.8$ and $T = 298$ K.

	Al-omega			Ga-omega		
Synthesis Temp. (K)	383	398	413	383	398	413
Adsorbate						
Water	20.45	18.10	17.30	17.50	14.89	15.3
n-butylamine	17.19	13.22	10.10	15.50	11.69	9.6
n-hexane	6.70	3.51	2.09	4.70	3.57	1.8
cyclohexane	6.50	3.33	2.25	4.61	2.27	1.8

The sorption of water, however, gives the measure of the hydrophilic/hydrophobic character of the product or also the measure of incorporation of trivalent species like Al^{3+} and Ga^{3+} in the silica matrix. n-Hexane, cyclohexane and n-butylamine (n-BA) are comparatively larger in size and they become occluded in the cavities of zeolites of crystallinity higher than 50%.

Table IV summarizes the sorption uptake (at $P/P_0 = 0.8$, 298 K) of water, n-hexane, cyclohexane and n-BA in fully crystalline samples of Al- and Ga-omega synthesised at different temperatures. The salient features of Table IV are as follows. The sorption uptakes are found to decrease with the increase in synthesis temperature. Since the gel SiO_2/M_2O_3 ratio and product SiO_2/M_2O_3 ratio (M = Al or Ga) are almost the same for all the samples; at least, water sorption uptake is not expected to change. The decrease in sorption uptake with the increase in synthesis temperature is consistent with the observed increase in the crystallite size. As the molecular size of the probe molecules increases, a decrease in sorption uptake with the increase in crystallite size becomes appreciable on account of their different packing in the zeolite voids. Ga-omega exhibits lower sorption uptake than its aluminium analog, on account of the larger crystallites of the former. Both the polar molecules like water and n-BA show higher sorption uptake than that for nonpolar molecules like n-hexane and cyclohexane. Polar molecules are expected to interact strongly with the sorption centres (extra framework cations) and may also lead to a close packing and hence may exhibit enhanced sorption uptake.

4. Conclusions

Zeolite Al-omega was synthesised hydrothermally using TMA-OH (25 wt.-% in methanol) in the temperature range of 383–413 K. The apparent activation energies for the process of nucleation and crystal growth were obtained from crystallisation kinetics. Zeolite Ga-omega was also hydrothermally crystallised at 398 K using TMA-OH as template. The incorporation of Ga in the omega framework was confirmed by chemical analysis, XRD, framework IR and solid state MAS

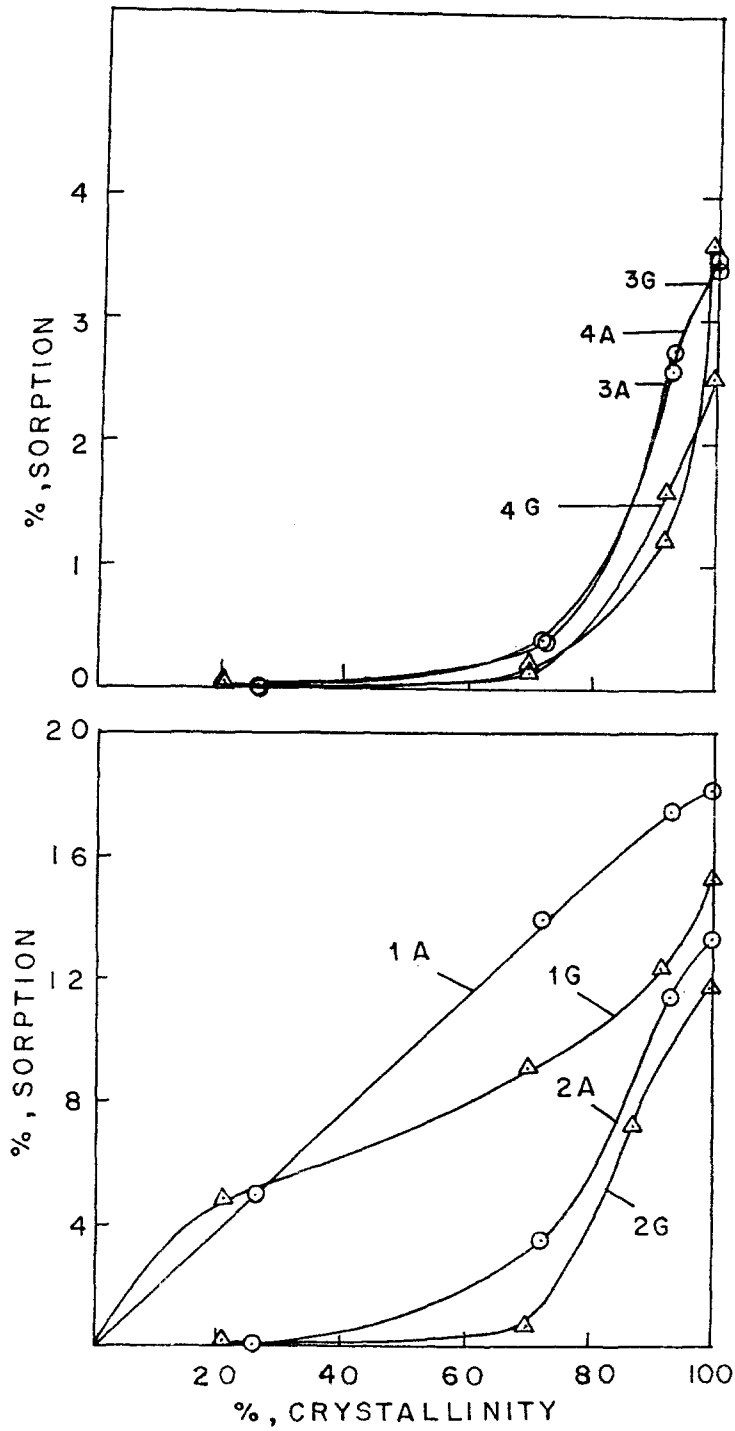

Fig. 7. Sorption uptake (wt.-%) as a function of degree of crystallinity at 398 K for Al-omega (1A) water, (2A) *n*-butylamine, (3A) *n*-hexane, (4A) cyclohexane and for Ga-omega (1G) water, (2G) *n*-butylamine, (3G) *n*-hexane and (4g) cyclohexane.

NMR spectra. The unit cell volume obtained from the XRD data for Ga-omega (2545 $Å^3$) was found to be higher than that (2519 $Å^3$) for Al-omega zeolite. The IR spectra of the Ga-omega shows a lower wavenumber for all the structure-sensitive vibrations, due to the incorporation of heavier Ga atoms, as compared to those of Al-omega. The ^{71}Ga MAS NMR spectrum confirms the tetrahedral coordination of Ga^{3+} species in the omega framework. Al-omega exhibited spherical crystallites (3 μm), whereas a cylindrical morphology (3.5–8.0 μm) was obtained for Ga-omega. Chemical analysis shows that the sodium occupancy in Ga-omega (90%) is higher than that in Al-omega (79%). The Al- and Ga-omega are stable up to a temperature of 1273 K. Sorption uptakes were found to be higher for Al-omega than for Ga-omega.

References

1. R.M. Barrer and H.Z. Villigier: *Kristallogr.* **128**, 352 (1969).
2. E. Galli: *Cryst. Struct. Commun.* **3**, 339 (1974).
3. R. Rinaldi, J.J. Pluth and J.V. Smith: *Acta Crystallogr.* **B 31**, 1603 (1975).
4. E.M. Flanigen and E.R. Kellberg: *Dutch Pat.* 6, 710, 729 (1968).
5. R. Aiello and R.M. Barrer: *J. Chem. Soc. A*, 1470 (1970).
6. J.F. Cole and H.W. Kouwenhoven: *Adv. Chem. Ser.* **121**, 583 (1973), Am. Chem. Soc., Washington DC.
7. A.J. Perrotta, C. Kibby, B.R. Mitchell and E.R. Tucci: *J. Catal.* **55**, 240 (1978).
8. J. Ciric: *French Pat.* 1 502 289 (1967), *U.S. Pat.* 3 923 639 (1975).
9. J. Ciric and L.J. Reid: *U.S. Pat.* 3 433 589 (1969).
10. F.G. Dwyer and P. Chu: *J. Catal.* **59**, 263 (1979).
11. A. Araya, T.J. Barber, B.M. Lowe, D.M. Sinclair and A. Varma: *Zeolites* **4**, 263 (1984).
12. R.M. Barrer: *Hydrothermal Chemistry of Zeolites*, Academic Press, London (1982), p. 251.
13. R. Szostak and T.L. Thomas: *J. Catal.* **100**, 555 (1986).
14. W.J. Ball, J. Dwyer, A.A. Garforth and W.J. Smith: *Stud. Surf. Sci. Catal.* **28**, 137 (1986).
15. J.M. Newsam and D.E.W. Vaughan: *New Developments in Zeolite Science and Technology*, Y. Murakami and J.W. Ward (Eds.) (1986), p. 459.
16. S. Hayashi, K. Suzuki, S. Shin, K. Hayamizu and O. Yamamoto: *Bull. Chem. Soc. Jpn.* **15**, 52 (1985).
17. G.N. Rao, V.P. Shiralkar, A.N. Kotasthane and P. Ratnasamy: *Molecular Sieves*, Vol. I, *Synthesis of Microporous Materials*, Ch. 13, M.L. Occelli and H.E. Robson (Eds.), Van Nostrand Reinhold, New York (1992), p. 153.
18. M.J. Eapen, K.S.N. Reddy, P.N. Joshi and V.P. Shiralkar: *J. Incl. Phenom.* **14**, 119 (1992).
19. G.H. Kuhl: *J. Inorg. Nucl. Chem.* **33**, 3261 (1971).
20. J.M. Newsam, R.H. Jasman and A.J. Jacobson: *Mat. Res. Bull.* **20**, 125 (1985).
21. D.E.W. Vaughan and K.G. Strohmaier: *Molecular Sieves*, Vol. I, *Synthesis of Microporous Materials*, Ch. 8, M.L. Occelli and H.E. Robson (Eds.), Van Nostrand Reinhold, New York (1992), p. 92.
22. P.N. Joshi, A.N. Kotasthane, V.P. Shiralkar: *Zeolites* **10**, 598 (1990).
23. F. Fajula, S. Nicolas, F.D. Renzo, C. Gueguen and F. Figueras: *Zeolite Synthesis*, ACS Symp. Series, Vol. 398, M.L. Occelli and H. Robson (Eds.) (1988), p. 493.
24. R. Szostak: *Molecular Sieves: Principles of Synthesis and Identification*, Van Nostrand Reinhold (1989), p. 320.
25. R. Szostak and T.L. Thomas: *J. Catal.* **101**, 549 (1986).
26. P. Massiani, F. Fajula and F. Figueras: *Zeolites* **8**, 322 (1988).
27. B. Chauvin, P. Massiani, R. Dutartre, F. Figueras and F. Fajula: *Zeolites* **10**, 174 (1990).
28. D.W. Breck, *Zeolite Molecular Sieves, Structure, Chemistry and Use*, John Wiley Interscience, New York (1974), p. 364.